

Effect of cobalt on the corrosion behaviour of amorphous Fe-Co-Cr-B-Si alloys in dilute mineral acids^(*)

I. Solomon* and N. Solomon**

Abstract

The aim of this paper was to investigate the effect of increasing cobalt content on the corrosion resistance of the Fe-Co-Cr-B-Si alloys in dilute mineral acids. The corrosion rates in 0.5N HCl, 1N HCl and 1N H₂SO₄ significantly decrease with an increase in cobalt content. The alloys with a larger amount of cobalt can passivate spontaneously. The high corrosion resistance of the Fe-Co-Cr-B-Si alloys is also due to the formation of chromium -enriched passive film. Generally, the corrosion resistance of chromium -bearing alloy is improved by alloying with various metalloids but it is lowered by addition of boron and silicon. The corrosion behaviour of the amorphous Fe_{75-x}Co_xCr₁B₇Si₁₇ alloys obtained by the melt-spinning technique was studied using gravimetric method. The best results were obtained with Fe₆₅Co₁₀Cr₁B₇Si₁₇ alloy. The studied amorphous alloy ribbons exhibit not only excellent physical properties which are useful for many electric and magnetic applications: magnetic sensors, power transformers, high frequency transformers, etc., but also a very good corrosion resistance which extend their application domain.

Keywords

Amorphous alloy; Corrosion; X-Ray diffraction; Alloying element; Passivation; Metalloid.

Efecto del cobalto en el comportamiento de la corrosión de aleaciones amorfas Fe-Co-Cr-B-Si en ácidos minerales diluidos

Resumen

Este trabajo presenta los resultados de la investigación sobre la resistencia a la corrosión de un nuevo sistema de aleaciones amorfas, p. ej., Fe-Co-Cr-B-Si. El comportamiento de la corrosión de aleaciones amorfas así como el de cualquier otra aleación cristalina puede ser determinado, en ambas, por factores internos (la estructura y composición de la aleación) y por factores externos (tipo medio agresivo, concentración y coeficiente pH). La falta de cristalinidad y de defectos específicos al estado de cristalinidad -limitaciones de grano, dislocaciones y segregaciones- aseguran una alta resistencia a la corrosión a las aleaciones amorfas, en lugar de ser termodinámicamente metaestables. La investigación se desarrolló a través del método gravimétrico en muestras de aleación amorfa Fe_{75-x}Co_xCr₁B₇Si₁₇ obtenidos por la técnica de centrifugado. Esta investigación muestra la influencia de la composición química de la aleación, por ejemplo, el porcentaje de cobalto y el medio de trabajo 0,5N HCl, 1N HCl y 1N H₂SO₄ en la resistencia a la corrosión. Los mejores resultados fueron obtenidos con Fe₆₅Co₁₀Cr₁B₇Si₁₇.

Palabras Clave

Materiales amorfos; Corrosión; Difracción de rayos X; Elemento de aleación; Pasivación; Metalloide.

1. INTRODUCTION

Electrochemical interest in metallic glasses aroused since their appearance. In 1974, Naka, Hashimoto and Masumoto brought into evidence both the corrosion resistance and the inertness in various aqueous electrolytes^[1-6]. It is believed that all sources of localized corrosion disappear in the absence of common structural defects such as the grain

boundaries, dislocations and segregations^[7-10]. Structure, chemical composition and material homogeneity are the factors influencing the electrochemical behaviour of amorphous alloys. Lack of sensitivity of an amorphous alloy to intergranular corrosion is apparently due to grain boundaries and segregations associated with them^[3 and 11-13]. A majority of amorphous alloys are passive in aqueous media. Considering the remarkable corrosion

^(*) Trabajo recibido el día 13 de Abril de 2009 y aceptado en su forma final del día 22 de Febrero 2010.

* Dunarea de Jos, Galati University, 47 Domneasca Street, 800008 Galati, Romania.

** Stefan cel Mare, Suceava University, 13 Universitii Street, 720229 Suceava, Romania.

resistance of iron, nickel, Co-based amorphous alloys it is important to explain the electrochemical action of metalloid elements (P, B and Si) as well as their combination with alloying elements (Cr, Mo and W)^[11 and 14].

The corrosion of metallic alloys is strongly influenced by alloying elements as well as by the microstructure. The preliminary study has revealed that the corrosion resistance of Fe, Ni, Cu, Co-based amorphous alloys in sulphate and chloride media is greatly affected by alloying with various additional elements such as Cr, Co, Mo, Ni or Nb^[10 and 15-17]. Similar to the effect observed for stainless steel, chromium is the essential element in forming the passive film^[6 and 16]. Increasing the chromium content increases the stability of the passive film. When certain amount of chromium is added, the surface film and spontaneous passivation often takes place by the formation of passive hydrated chromium oxy-hydroxide film^[13 and 16-20].

Analysis of the surface by different methods allows the determination of the composition of passive layers and the distribution of the alloying elements. Other alloying elements such as cobalt can influence the effectiveness of chromium in forming or maintaining the passive film. The passivation process in the amorphous alloys is more efficient with increasing cobalt content because of the excellent protective effectiveness of cobalt oxides^[10, 18 and 21].

The effect of chrome on the corrosion resistance of amorphous alloys is higher than that in the case of crystalline alloys^[2, 19, 22 and 23]. Jayaraj *et al.*^[8] have shown that, for identical chrome content, Fe-based amorphous alloys have superior corrosion properties than AISI316L stainless steels^[24 and 25].

According to Lekatou *et al.*^[3] the amorphous alloys passivating ability and consequently their corrosion behaviour is significantly affected by metalloid elements (B, C, P, Si) contained in the alloys. Referring to boron and silicon contained in amorphous alloys they tend to form borate and silicate in the film surface with a consequent decrease in enrichment of protective oxy-hydroxide in the film^[13, 16 and 20]. Particularly, boron has been found to participate in both passive and active corrosion products. The addition of silicon to the alloy forms a chromium – silicate and do not enhance the quality of the passive film.

The behaviour of Fe-Cr-P ternary alloys in aggressive media such as 1N HCl as compared to stainless steel is obvious. The efficiency of simultaneous alloying with chrome and phosphorus is superior to that of chrome and boron and consequently should be emphasized. The FeCr₁₀P₁₃C₇ amorphous alloy passivates spontaneously in an

aggressive medium. It has been found that phosphorus improves the corrosion resistance of amorphous alloys and in the same time the passivation process being incorporated as phosphates in the passive film^[6 and 16].

The previous studies^[2, 18, 22 and 26] showed that the optimum enrichment in chrome in the case of passive films attains a maximum value with amorphous alloys showing 95 % cations as compared with noticeable values in the case of conventional ferrite steels showing 58-75 % cations. Comparison of the effect of other amorphizing elements underlines the special position phosphorus holds. In the case of steels including phosphorus, boron or silicon the above mentioned amorphizing elements cause the formation of a chromium borate or silicate which limits the percentage of this element available for the formation of the protective film of chromium hydroxide monohydrate^[27-29].

2. EXPERIMENTAL PROCEDURE

Alloy ingots of Fe_{75-x}Co_xCr₁B₇Si₁₇ (where: x=1, 4, 7, and 10 % Co) system were prepared from a mixture of pure Fe, Co, Cr, B and Si metals (purity ≥ 99.9 %) by arc melting technique in a purified argon atmosphere. Amorphous alloy ribbons were obtained by the melt-spinning technique which consists in impinging a jet of molten alloy on the outer surface of a rotating copper wheel. The rotational speed of the dynamic equilibrated wheel was kept at 2100 rpm. The amorphous nature of the samples was confirmed by X-ray diffraction studies using Cu- K \cdot radiation. The diffraction pattern of studied ribbon samples is characterized by the typical halo indicating that the as-cast samples are in the amorphous state^[30] (Fig. 1). The *Mössbauer* spectrum of the amorphous Fe₇₁Co₄Cr₁B₇Si₁₇ alloy, done at room temperature (Fig. 2), is typically also for a quenched sample in amorphous state.

Microhardness of ribbons in as cast state has been measured using *Vickers* method with a 50 g load for comparative calculus. In figure 3, it can be noticed that the microhardness of amorphous alloys increases with the increasing of cobalt percentage. It is probably due^[30] to the formation of a more dense ribbon microstructure as a result of cobalt clusters formation prior to the commencement of the melt quenching on the roller. The cobalt clusters induce their preferential crystallization in a phase rich in iron and chrome. In this way the cobalt clusters act in the same way as an annealing heat treatment.

For corrosion behaviour characterization the alloys were tested in order to find out the weight loss in

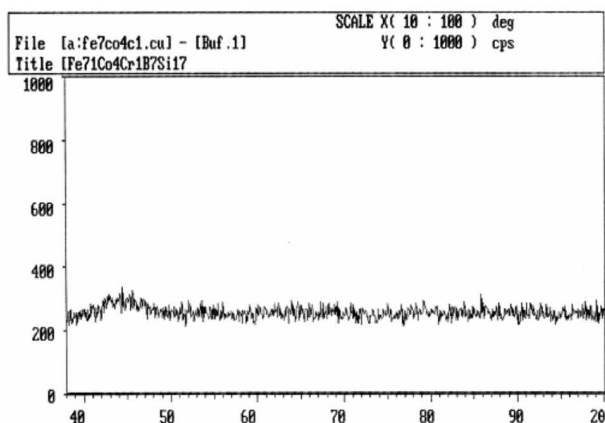


Figure 1. Fe₇₁Co₄Cr₁B₇Si₁₇ alloy X-ray diffraction diagram.

Figura 1. Diagrama de la difracción con rayos X de la aleación Fe₇₁Co₄Cr₁B₇Si₁₇.

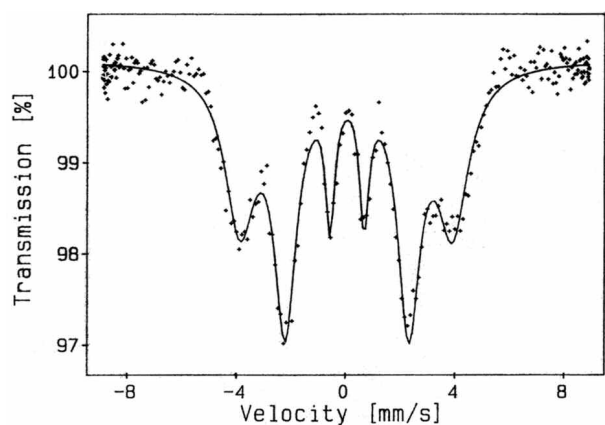


Figure 2. Mössbauer spectrum of Fe₇₁Co₄Cr₁B₇Si₁₇ alloy in as cast state.

Figura 2. Espectro de Mössbauer de la aleación amorfa de Fe₇₁Co₄Cr₁B₇Si₁₇ en estado inicial.

three media, namely 1N H₂SO₄, 0.5N and 1N HCl. The losses were recorded for a 4 hour interval when weights were performed every 30 minutes. The corrosion rate for each time interval was determined by means of the following equation:

$$v_{\text{cor}} = \frac{\Delta m}{S \cdot t} \times 10^{-1} \text{ [kg/m}^2 \cdot \text{h]} \quad (1)$$

where,

- v_{cor} – corrosion rate;
- Δm – mass loss;
- s – sample surface;
- t – test duration,

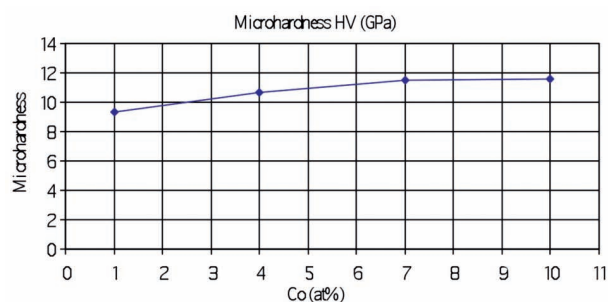


Figure 3. Microhardness versus cobalt content of the Fe_{75-x}Co_xCr₁B₇Si₁₇ amorphous alloys.

Figura 3. Micro dureza vs contenido de cobalto de las aleaciones amorfas Fe_{75-x}Co_xCr₁B₇Si₁₇.

and penetration coefficient,

$$i_p = \frac{v_{\text{cor}}}{\rho} \times 8.76 \cdot 10^{-3} \text{ [m/year]} \quad (2)$$

where,

ρ – material density.

The samples were very thin ribbons with thickness between 25 and 32 μm and 2 mm the width, having a very large surface in contact with the corrosive agent. Before being weighed with a digital analytical balance, samples were degreased in acetone, washed in distilled water and then dried in air. Electrolytes of 1N H₂SO₄, 0.5N HCl and 1N HCl solutions open to air were used at room temperature (about 298 K). Mass loss of the amorphous alloys ribbons after immersion in the above mentioned solutions was measured for estimating the corrosion rates. After the immersion test, surfaces of the alloy specimens were observed by optical microscope.

3. RESULTS AND DISCUSSION

In this section some of the experimental research results regarding to the corrosion resistance of the above mentioned alloys will be presented. The air side surface (freely solidified) and the wheel side surface (solidified in contact with the rotating support) of the amorphous ribbons were studied under an optical microscope. The wheel side surface shows very small air pockets randomly distributed with varying size produced by gases entrapped by the liquid metal jet during the production process. The samples also show asperities (roughness) on the air side

surface^[7, 26 and 31]. Figure 4, obtained by optical microscope, shows the above stated aspects.

The surface of the sample was also analyzed after the corrosion test. The ribbon surface contacting the rotating support shows a higher corrosion resistance than the surface in the opposite side. This can be explained by the cooling process of these two surfaces at different cooling rates during the solidification process. Due to a lower cooling rate of the air side surface crystalline nuclei could form, but this process was not confirmed through the X-ray diffraction^[7]. The present study has been performed in order to investigate the effect of increasing cobalt content on the corrosion resistance of the series of $\text{Fe}_{75-x}\text{Co}_x\text{Cr}_1\text{B}_7\text{Si}_{17}$ amorphous alloys.

The amorphous metallic alloys are thermodynamically unstable. The corrosion behaviour in the case of the amorphous alloys as well as in that of any crystalline alloys may be influenced both by internal factors (the alloy composition, the type of the components, the presence of the metalloids) and by external ones (aggressive medium pH-coefficient and composition). Irrespective of the corrosive medium, the amorphous alloys have a better

and better behaviour proportionally with increasing cobalt content, which is obvious in figures 5-6.

The histograms of figure 5 show the dependence of corrosion rate of $\text{Fe}_{75-x}\text{Co}_x\text{Cr}_1\text{B}_7\text{Si}_{17}$ alloys in (a) 1N H_2SO_4 , (b) 1N HCl and (c) 0.5N HCl solutions versus the cobalt content. The variation of corrosion resistance expressed by the penetration coefficient can be noticed in figure 6. According to figure 5a, in sulphate solution the average corrosion rate remain substantially constant with increasing cobalt content. In chloride medium (Fig. 5 b) and 5 c)) it is observed that the average corrosion rate decreases with increasing cobalt content but it remain almost constant for different immersion periods. However, the chloride solution shows a lower aggressivity than sulphate media and consequently the average corrosion rate is more than twice lower than in sulphate one, figure 6.

Quantitative analysis of the elements dissolved in 0.5 N and 1N HCl solutions revealed the following (Figs. 5 b) and 5 c)):

- In more aggressive solutions alloys with low Co content the dissolution rates are close to those of the nominal alloys (i.e., $\text{Fe}_{74}\text{Co}_1\text{Cr}_1\text{B}_7\text{Si}_{17}$).

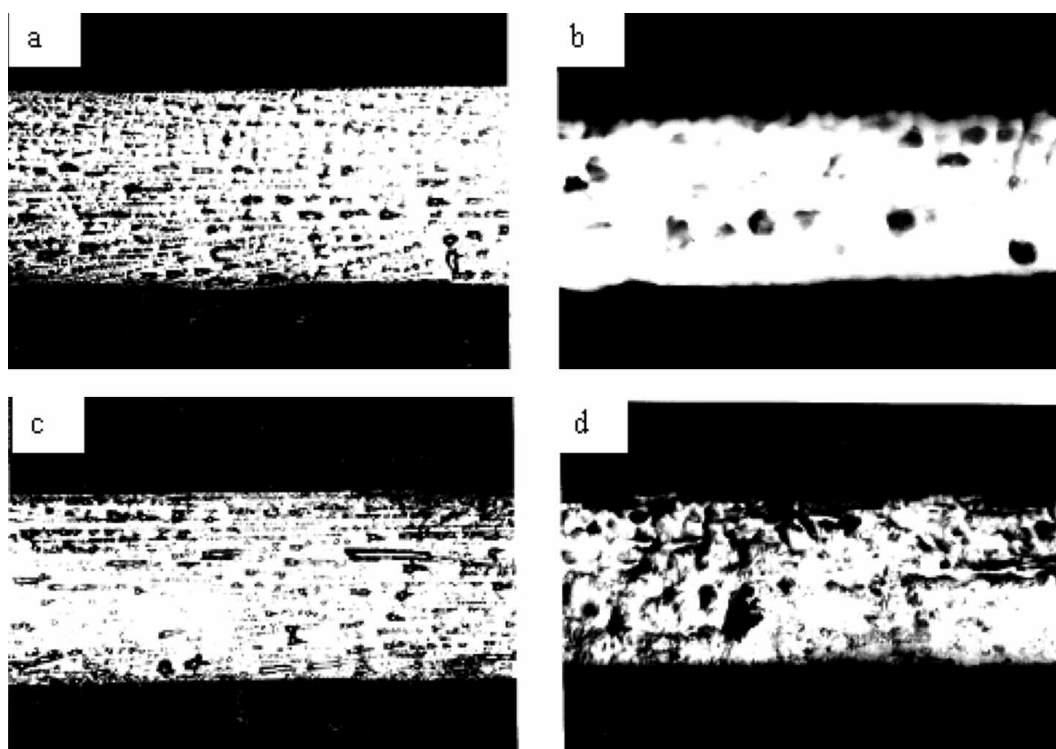


Figure 4. Surface morphology of the $\text{Fe}_{71}\text{Co}_4\text{Cr}_1\text{B}_7\text{Si}_{17}$ amorphous ribbons (a, c) wheel side and (b, d) air side surfaces (a, b) before and (c, d) after corrosion.

Figura 4. Morfología de la superficie de los listones amorfos de $\text{Fe}_{71}\text{Co}_4\text{Cr}_1\text{B}_7\text{Si}_{17}$ (a, c) lado de la rueda y (b, d) superficies de aire de lado (a, b) antes y (c, d) después de la corrosión.

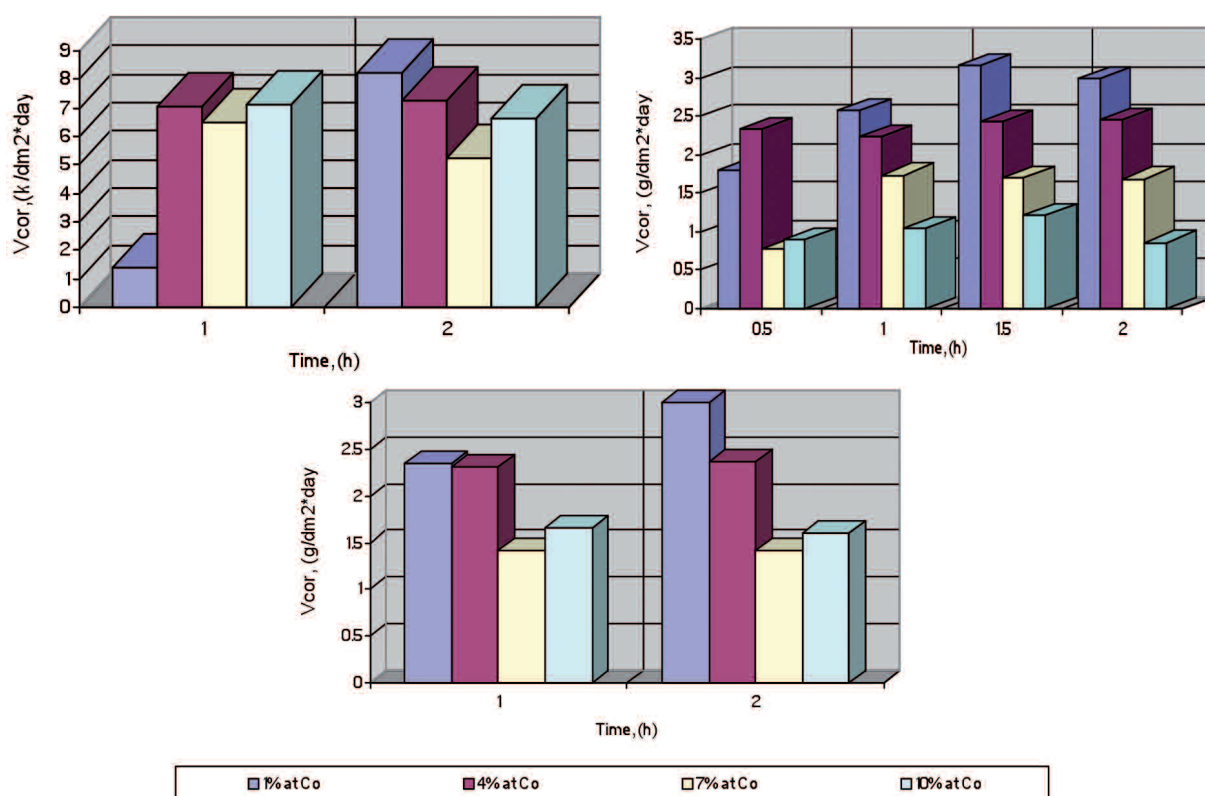


Figure 5. Histograms showing the dependence of corrosion rate of Fe_{75-x}Co_xCr₁B₇Si₁₇ alloys in (a) 1N H₂SO₄, (b) 1N HCl and (c) 0.5N HCl media versus the cobalt content.

Figura 5. Histogramas mostrando la dependencia de la tasa de corrosión de la aleación Fe_{75-x}Co_xCr₁B₇Si₁₇ en (a) 1N H₂SO₄, (b) 1N HCl y (c) 0.5N HCl media sobre el contenido de cobalto.

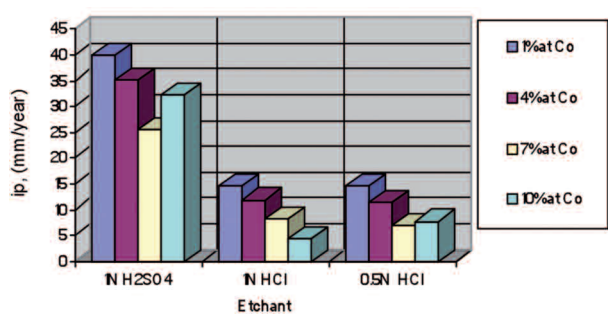


Figure 6. Variation of penetration coefficient depending on the cobalt concentration and the nature of the aggressive medium.

Figure 6. Variación del coeficiente de la penetración dependiendo de la concentración de cobalto y de la naturaleza del medio agresivo.

— In almost neutral solutions alloys with high Co content the dissolution rates are perceptibly different from those of the nominal compositions.

At high percentage the cobalt forms a superficial protective film, probably a hydrated oxide, which prevents further dissolutions^[32-34]. The corrosion behaviour of the metallic glasses primarily depends on the character of the alloying elements. The corrosion resistance of Fe-Co-Cr-B-Si alloys significantly increases with decreasing iron content. Consequently, the corrosion resistance of Fe_{75-x}Co_xCr₁B₇Si₁₇ amorphous alloys is improved as the cobalt replaces iron. This effect may be explained by the behaviour of cobalt itself. Cobalt may be characterized by a low corrosion rate in neutral aqueous solutions, without oxidants, and a low corrosion rates in acid solutions^[18].

Higher corrosion resistance of amorphous alloys than that of crystalline ones is attributable to their structure, chemical composition and material homogeneity. It is known that in the case of crystalline alloys, mono-phase alloys have a better corrosion resistance than bi or multi phases alloys. Good corrosion resistance of single phase metallic alloys is often ascribed to their structural and compositional homogeneity^[12 and 13]. However, in the

case of crystalline structure corrosion often occurs preferentially at grain boundaries and second phase particles. Since they do not have grain boundaries, segregates or crystalline defects which may act as corrosion initiation sites, amorphous alloys are expected to have better corrosion resistance than their metallic constituents^[8].

Good corrosion resistance of amorphous alloys is also linked to the ability of these alloys to form supersaturated solid solution in one or more alloying elements. These alloying elements available in solid solution may be incorporated into the oxide film to enhance its passivity^[18, 20 and 26].

The most effective alloying addition in improving the corrosion resistance of amorphous alloys in acidic solutions is chromium. Chromium is an essential element in forming the passive film during corrosion process of Fe-based amorphous alloys in sulphate and chloride environments. The passive film is essentially composed by Cr_2O_3 covering Fe_2O_3 . However, the metalloid elements such as boron and silicon contained in the Fe-Co-Cr-B-Si system and which form borate and silicate in the film surface do not have a positive effect on the passivating ability of amorphous alloys.

Figure 7 shows the results of quantitative analysis for iron and cobalt dissolved in the 0.5N HCl solution. The data in the table related to the total weight losses during the corrosion process, refer only to the iron and cobalt percentage variation as components of the $\text{Fe}_{75-x}\text{Co}_x\text{Cr}_1\text{B}_7\text{Si}_{17}$ amorphous alloys.

Immersion test of the $\text{Fe}_{75-x}\text{Co}_x\text{Cr}_1\text{B}_7\text{Si}_{17}$ amorphous alloys in 0.5N HCl solution has revealed the effect of the substitution of iron with cobalt. It is obvious that the cobalt shows a slower active dissolution rate than iron^[17]. In 0.5N HCl solution the iron dissolution rate is almost twice bigger than the cobalt dissolution rate. The percentage of iron dissolved in 0.5N HCl solution rapidly decreased with

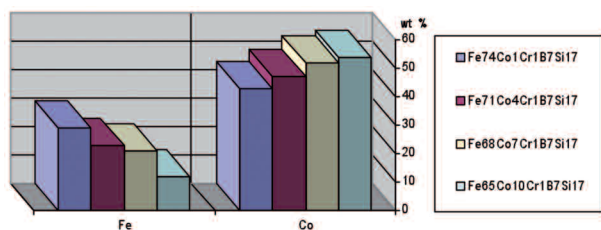


Figure 7. Variation in iron and cobalt dissolved in the 0.5N HCl etchant.

Figure 7. Variación en hierro y cobalto disueltos en 0.5N HCl.

increasing cobalt content, but in the same time the percentage of cobalt dissolved in 0.5N HCl solution slightly increased with increasing cobalt content of the $\text{Fe}_{75-x}\text{Co}_x\text{Cr}_1\text{B}_7\text{Si}_{17}$ amorphous alloys.

The present study underlines the importance of the corrosive medium and its concentration. The Fe-Co-Cr-B-Si alloys displayed inferior corrosion resistance in sulphuric acid and its penetration coefficient ranges between 20 and 40 mm/year, as compared to their behaviour in hydrochloric acid in which the penetration coefficient is between 4 and 14 mm/year. When the samples were kept in 1N hydrochloric acid for four hours practically the penetration coefficients are identical with those kept in 0.5N hydrochloric acid for two hours. The passivation of amorphous alloys increases with increasing of HCl concentration.

4. CONCLUSIONS

Taking into account the above mentioned results the following conclusions can be drawn:

- $\text{Fe}_{75-x}\text{Co}_x\text{Cr}_1\text{B}_7\text{Si}_{17}$ (where, $x=1, 4, 7,$ and 10% Co) amorphous alloys exhibit an increased micro-hardness and a high corrosion resistance in dilute mineral acids with an increase in cobalt content. At high percentage the cobalt forms a thin protective film which prevents further corrosion.
- Chromium is an essential element in forming the passive film during corrosion process of $\text{Fe}_{75-x}\text{Co}_x\text{Cr}_1\text{B}_7\text{Si}_{17}$ (where, $x=1, 4, 7,$ and 10% Co) amorphous alloys in sulphate and chloride environments.
- The corrosion resistance of the ribbons in the hydrochloric acid environments varies with solution concentrations. The penetration coefficients are identical when samples were kept in 1N HCl for 4 h with those recorded when samples were kept for 2 h in 0.5N HCl. It means that the amorphous alloy becomes more passive when the HCl concentration increases.
- The ribbon wheel side surface shows a higher corrosion resistance than the surface in the opposite side. This behaviour is the result of some structural differences between air side (free of grain boundaries, second-phase particles) and wheel side ribbon surfaces due to the cooling process at different cooling rates.

REFERENCES

- [1] M. Naka, K. Hashimoto and T. Masumoto, *J. Japan Inst. Metals* 38 (1974) 835-841.
- [2] F. Dabosi, Colloque FORMATION, Societe Francaise de Metallurgie, INP, Toulouse, Tarbes, 1985.
- [3] A. Lekatou, A. Marinou, P. Patsalas and M.A. Karakassides, *J. Alloys Compd.* 483 (2009) 514-518.
- [4] J. Jayaraj, K.B. Kim, H.S. Ahn and E. Fleury, *Mater. Sci. Eng. A* 449-451 (2007) 517-520.
- [5] S. Pang, C. Shek, T. Zhang, K. Asami and A. Inoue, *Corros. Sci.* 48 (2006) 625-633.
- [6] I. Chattoraj, S. Baunack, M. Stoica and A. Gebert, *Mater. Corros.* 55 (2004) 36-42.
- [7] R.S. Dutta and G.K. Dey, *Bull. Mater. Sci.* 26 (2003) 477.
- [8] J. Jayaraj, Y.C. Kim, K.B. Kim, H.K. Seok and E. Fleury, *Sci. Technol. Adv. Mater.* 6 (2005) 282-289.
- [9] D. Zander, B. Heisterkamp and I. Gallino, *J. Alloys Compd.* 434/435 (2007) 234-236.
- [10] R. Raicheff and V. Zaprianova, *J. Univ. Chem. Tech. Metall.* 44 (2009) 61-65.
- [11] Z.L. Long, C.T. Chang, Y.H. Ding, Y. Shao, P. Zhang, B.L. Shen and A. Inoue, *J. Non-Crys. Solids* 354 (2008) 4609-4613.
- [12] R. Zallen, *The Physics of Amorphous Solids*, John Wiley & Sons, 1998.
- [13] H. H. Liebermann, *Rapidly solidified alloys: processes, structures, properties, applications*, Marcel Dekker, New York, 1993.
- [14] H.G. Kim, M. S. Kim and W. N. Myung, *J. Korean Phys. Soc.* 49 (2006) 1.630-1.634.
- [15] C. Qin, W. Zhang, K. Asami, N. Ohtsu and A. Inoue, *Acta Mater.* 53 (2005) 3.903-3.911.
- [16] T. Masumoto and K. Hashimoto, *J. Phys. C* 8 (1980) 894-900.
- [17] FF Marzo, A.R. Pierna, J. Barranco, A. Lorenzo, J. Barroso, J.A. García y A. Pérez, *J. Non-Crys. Solids* 354 (2008) 5.169-5.171.
- [18] E. Angelini, C. Antonione, M. Baricco, P. Bianco, F. Rosalbino and F. Zucchi, *Werkst. Korros.* 44 (1993) 98.
- [19] Z. Long, Y. Shao, G. Xie, P. Zhang, B. Shen and A. Inoue, *J. Alloys Compd.* 462 (2008) 52-59.
- [20] P. Marcus, *Corrosion mechanisms in theory and practice*, Marcel Dekker, New York, 2002.
- [21] A. Altube and A.R. Pierna, *Electrochim. Acta* 49 (2004) 303-311.
- [22] E. Angelini, C. Antonione, M. Baricco, P. Bianco, F. Rosalbino and F. Zucchi, *Metallurgia Italiana* 83 (1991) 671.
- [23] Z.L. Long, Y. Shao, X.H. Deng, Z.C. Zhang, Y. Jiang, P. Zhang, B.L. Shen and A. Inoue, *Intermetallics* 15 (2007) 1.453-1.458.
- [24] E. Fleury, J. Jayaraj, Y.C. Kim, H.K. Seok and K.Y. Kim and K.B. Kim, *J. Power Sources* 159 (2006) 34-37.
- [25] J. Jayaraj, Y.C. Kima, K.B. Kima, H.K. Seok and E. Fleury, *J. Alloys Compd.* 434/435 (2007) 237-239.
- [26] S. M. Gravano, S. Torchio, F. Mazza, E. Angelini and M. Baricco, *Corros. Sci.* 33 (1992) 1227.
- [27] M. Fujiwara, K. Takanashi, M. Satou, A. Hasegawa, K. Abe, K. Kakiuchi and T. Furuya, *J. Nucl. Mater.* 329/333 (2004) 452-456.
- [28] A.S. Hamada, L.P. Karjalainen, M.C. Somani, *Mater. Sci. Eng. A* 431 (2006) 211-217.
- [29] Y. S. Choi, J. J. Shim and J. G. Kim, *J. Alloys Compd.* 391 (2005) 162-169.
- [30] I. Solomon, *PhD Thesis*, University of Galati, 1998.
- [31] M. Magrini and P. Matteazzi, *J. Mater. Chem. Phys.* 13 (1985) 71.
- [32] A. Dhawan, S. Roychowdhury, P. K. De and S. K. Sharma, *Bull. Mater. Sci.* 26 (2003) 609.
- [33] V. Schroeder and R. O. Ritchie, *Acta Materialia* 54 (2006) 1785.
- [34] J. R. Scully, A. Geber and J. H. Payera, *J. Mater. Res.* 22 (2007) 302.